Miocene topography and bathymetry update. 2013.

Herold, N.

- Appendix A Miocene vegetation from *Herold et al.* [2011] mapped onto new topography.

- Appendix B Miocene river transport directions based on local topographic gradients.

The middle Miocene topography released in 2008 [*Herold et al.*, 2008] was based on rotated polygons cut from ETOPO2[1] and rotated to 15 Ma coordinates using the plate rotation model of *Müller et al.* [2008a]. The bathymetry in this dataset was based on a reconstruction for 15 Ma [*Müller et al.*, 2008b]. The modern topography was modified in areas known to have been significantly different to the present based on paleo-elevation proxies. Most notably this included the Tibetan Plateau, Andean Cordillera, North and South America and the ice-sheets [*Herold et al.*, 2008]. This approach takes advantage of the fact that over the vast majority of the world, tectonic and topographic change since the Miocene has been small and thus broad adjustments to modern topography can be considered sufficient for representing this period, with the added benefit of maintaining some level of roughness which is lost (or artificially created) when creating topographic datasets from scratch [e.g. *Markwick*, 2007]. However, some clear shortcomings are evident in our Miocene dataset, some of which were accounted for in subsequent revisions [c.f. Fig. 1 *Herold et al.*, 2011] such as elevation of the northern European continental shelf to above sea-level.

Below I describe changes made in the most recent revision of this dataset (available online at XXXX), consistent with available literature. The basis for this revision is the 0.5 x 0.5 degree dataset described in *Herold et al.* [2008]. The original 2008 and revised 2013 dataset are shown in Figure 1.

The Greenland-Scotland Ridge (GSR) was likely shallow or above sea-level during the early to middle Miocene, with the exception of the Faroe-Shetland Channel which was relatively deep [*Poore et al.*, 2006]. Such details are not reconstructed by the method of *Müller et al.* [2008b] given the generic workflow which utilises an age-depth relationship, sediment deposition and Large Igneous Province (LIP) emplacement. Consequently in the 2008 dataset the GSR was almost absent and Iceland was below sea level, having potentially large implications for deep water formation [*Herold et al.*, 2012; *Robinson et al.*, 2011]. To correct this we implement a shallow (-100 m) GSR with a deep Faroe-Shetland Channel (~ -4,500 m to be consistent with surrounding bathymetry). Based on fossil flora Iceland is known to have been sub-areal in the middle Miocene [*Denk et al.*, 2005; *Grímsson et al.*, 2007] and thus is made so here.

While *Müller et al.* [2008b] implement LIPs there is some error associated with their methods. For the Miocene the estimated depths of some LIPs can be checked against foraminifera-based depth estimates from deep sea drilling data. Accordingly, based on drilling reports the Madagascar Ridge, Mascarene Ridge and Kerguelen Plateau are adjusted to approximately 900, 700 and 2000 m depth respectively.

---

[1] http://www.ngdc.noaa.gov/mgg/fliers/01mgg04.html

Australian geography is adjusted to suit more the paleogeography established by *Langford et al.* [1995], namely marine transgressions in the southwest and southeast of the continent. The topography of Papua New Guinea was substantially reduced (to about 30% of the modern) given that the central mountain chain of the island did not uplift until the latest Miocene [*van Ufford and Cloos*, 2005].

The Amazon River is removed in our revised dataset. Evidence suggests the early Miocene Amazon reflected a "mega-wetland" which drained into the Caribbean, switching its drainage channels toward the Atlantic in the middle to late Miocene [*Hartley*, 2003; *Hoorn et al.*, 2010; *Shephard et al.*, 2010 and references therein]. Based on this data we choose to represent the Amazon using a "wetland" plant functional type in our vegetation input, though individual modellers may choose to represent the Amazon by changing the land mask to ocean at appropriate grid cells. A marine incursion in southern South America was also implemented in our dataset based on Markwick [2007].

The Panama gateway was likely open by the early-middle Miocene [see *Molnar*, 2008 for a review], though contradictory evidence exists suggesting no deep passage by 15 Ma [*Montes et al.*, 2012]. We choose a geography consistent with that of *Iturralde-Vincent* [2006], leaving only a deep meridional channel between the Pacific and Atlantic Oceans.

The Tethys and Mediterranean was re-modelled based on the geographic outline of *Karami* [2011], which was derived from *Meulenkamp and Sissingh* [2003]. This is a significant improvement over the "flooded Europe" implemented originally. The bathymetry of the Miocene Tethys Ocean is largely unknown, though suggestions exist [*Hüsing et al.*, 2009; *Meulenkamp and Sissingh*, 2003]. We implement somewhat deep bathymetry from the Strait of Gibraltar into the central Mediterranean, qualitatively consistent with *Meulenkamp and Sissingh* [2003] (Fig. 1b).

Perhaps the most significant improvement in this revised Miocene topographic/bathymetric dataset is the treatment of the Greenland and Antarctic ice-sheets. While the Cenozoic history of the Antarctic ice-sheet is ambiguous there is broad agreement that between the Eocene-Oligocene Transition (~34 Ma) and Middle Miocene Climate Transition (~14 Ma) the East Antarctic ice-sheet experienced significant fluctuations in volume and extent, whereas the West Antarctic Ice Sheet was likely non-existent or insignificantly small [*Cramer et al.*, 2011; *Pekar and DeConto*, 2006; *Zachos et al.*, 2001]. *Pekar and DeConto* [2006] estimate early Miocene ice volume to be 25 – 70% of the modern East Antarctic Ice Sheet (the contribution of the modern EAIS is equal to ~60 m sea-level rise after isostatic rebound). *Cramer et al.* [2011] recently calculated a more conservative ice-volume decrease for the Miocene, with their minimum predicted Miocene ice-volume ~55% of the present (based on a sea-level rise of ~30 m above present, compared to ~65 m for all ice-sheets). We choose to implement an ice-volume and sea-level rise consistent with extreme warmth in the Miocene. Our Antarctic topography is derived from a combination of two datasets. For the basis of our Antarctic topography and ice-sheet mask we utilise ice-sheet model output provided by David Pollard (personal comms), established using the same methodology in *Pollard and DeConto* [2009]. This simulated ice-sheet is underlain by modern bedrock and consists of approximately ~6.5 million km^3 of ice, compared to the modern Antarctic ice-sheet volume of ~27 million km^3 [*Fretwell et al.*, 2012]. The majority of this simulated ice resides in East Antarctica. For West-Antarctica we apply a modification to this

topography as follows: for each grid cell we utilise an ANTSCAPE derived dataset (produced as a sum of 40% Eocene maximum topography [Figure 5 *Wilson et al.*, 2012] and 60% modern bedrock) where this dataset is higher than our base topography. This is done in light of the suggestion that West Antarctic bedrock was higher than present at the Eocene-Oligocene Transition [*Wilson and Luyendyk*, 2009] and thus probably lay somewhere between modern and Eocene-Oligocene elevations during the Miocene. For the Greenland ice-sheet we utilise a simulated ice-sheet distribution based on work by Aisling Dolan for the Pliocene ice-sheet modelling intercomparison project (personal comms). This ice-sheet was simulated under 560 ppmv CO_2 and a mean Pliocene orbit, and has a volume of ~0.294 million km^3 (compared to 2.6 million km^3 at present [*Weidick et al.*, 1995]). The difference in insolation from a mean Pliocene and Miocene orbit is small (and is smaller than the difference between the present and Miocene orbit), thus we believe this ice-sheet to be an adequate representation for the Miocene Climatic Optimum. We note that evidence for significant Greenland ice-sheets prior to the Pleistocene is scarce; evidence exists for some ice in the Eocene [Eldrett et al., 2009] though these were not likely significant in size. Thus, like our Antarctic ice-sheet, this ice-volume is subject to some extent by personal preference. In total, our global Miocene ice-volume is ~6.8 million km^3, compared to a global (Antarctica+Greenland) modern volume of 29.6 million km^3 [*Fretwell et al.*, 2012; *Weidick et al.*, 1995]. Sea-level change is left at 50 m above present as per *Herold et al.* [2008] and is consistent with the 65 m sea-level contribution from all of the modern ice-sheets and the 6.8 million km^3 volume of our Miocene ice-sheets.

**Figure 1.** a) The original 0.5x0.5 degree dataset from *Herold et al.* [2008]. b) the revised dataset described in this document. Major regions of change include the Greenland and Antarctic ice-sheets and the Tethys Sea.

z ()

Data Min = -5270.14, Max = 4700.00

topo ()

Data Min = -5000.00, Max = 5000.00
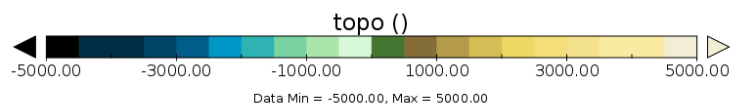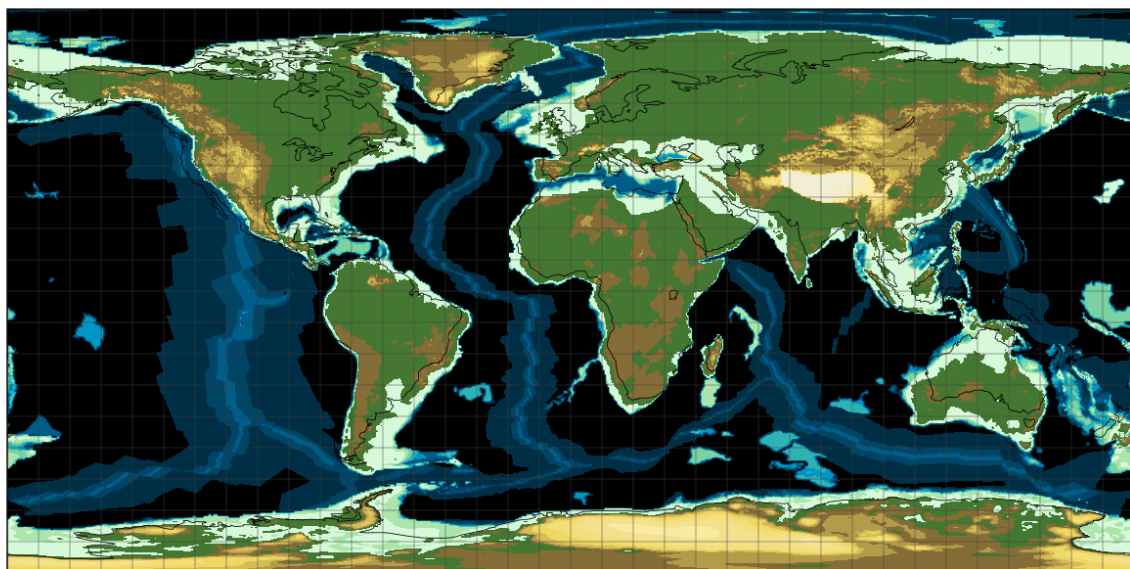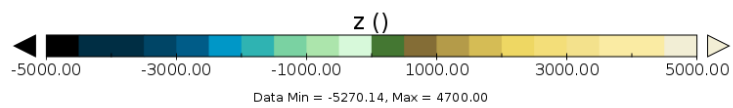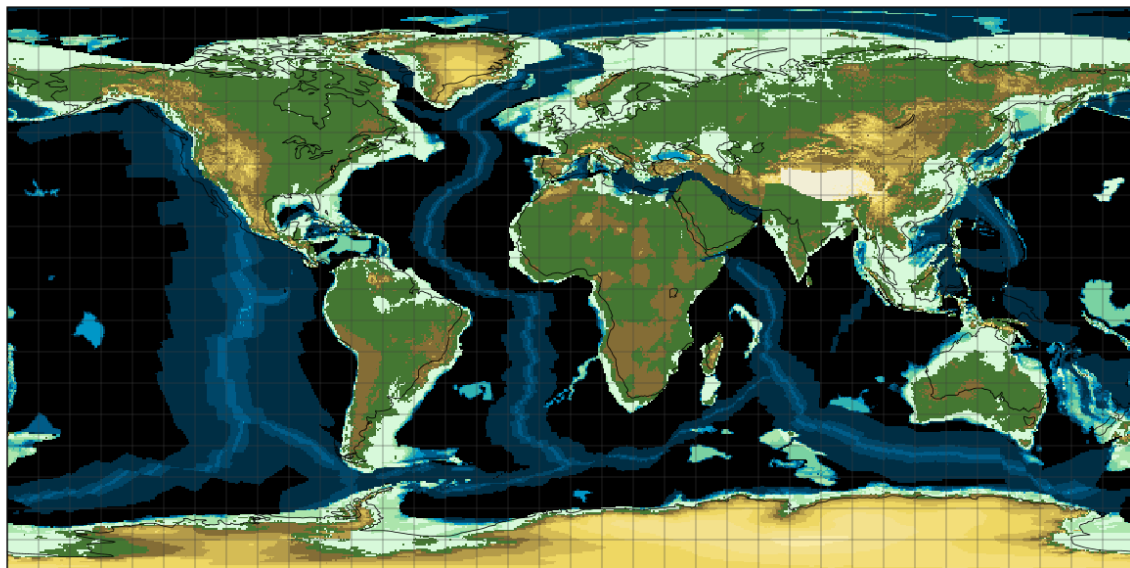
Appendix A – Miocene vegetation

Miocene vegetation used in *Herold et al.* [2011], based mostly off *Wolfe* [1985], mapped onto the revised topography described in this document. Topography is interpolated to 2x2 degrees resolution and 'tweaked' according to model requirements before input into the model, thus the LSM biome map below is on a 2x2 degree map that is used as input into the CESM model set up. Note that a few changes have been made to the placement of biomes, e.g. the Amazon basin now consists of a "mega wetland". For the plant functional types associated with each biome number indicated in the figure below, see paleo_mkraw_ccsm4_public_sed.F90 in the paleo_mkraw tool.

LSM Biomes

Data Min = 0.00, Max = 29.00
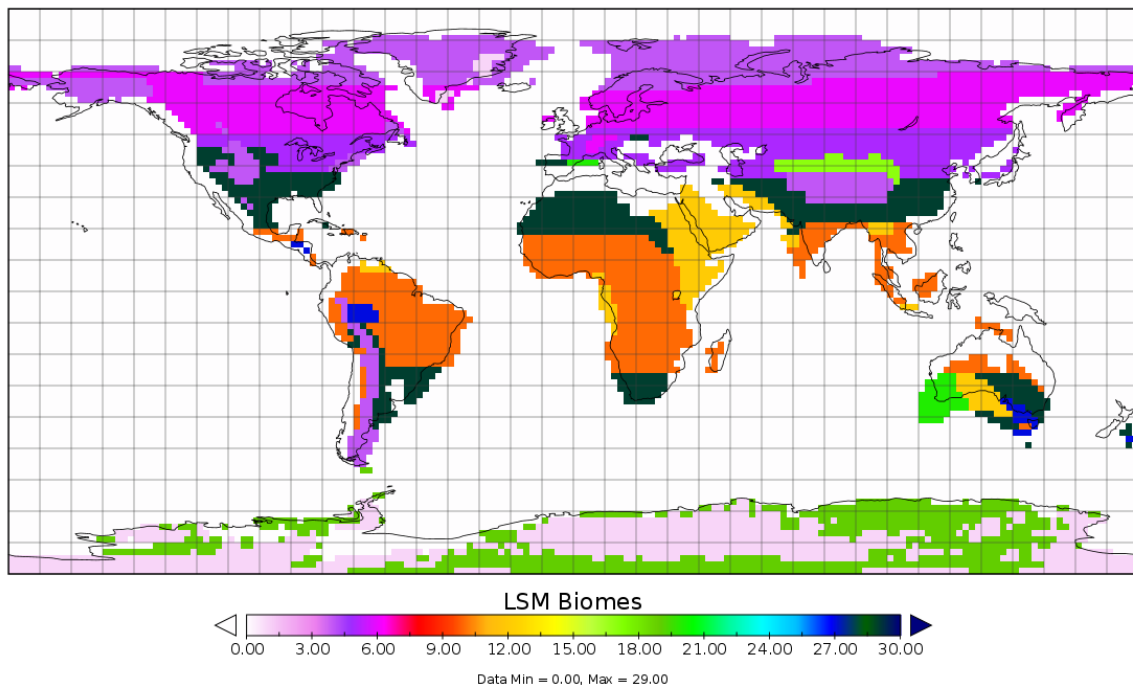
Appendix B − Miocene river runoff directions
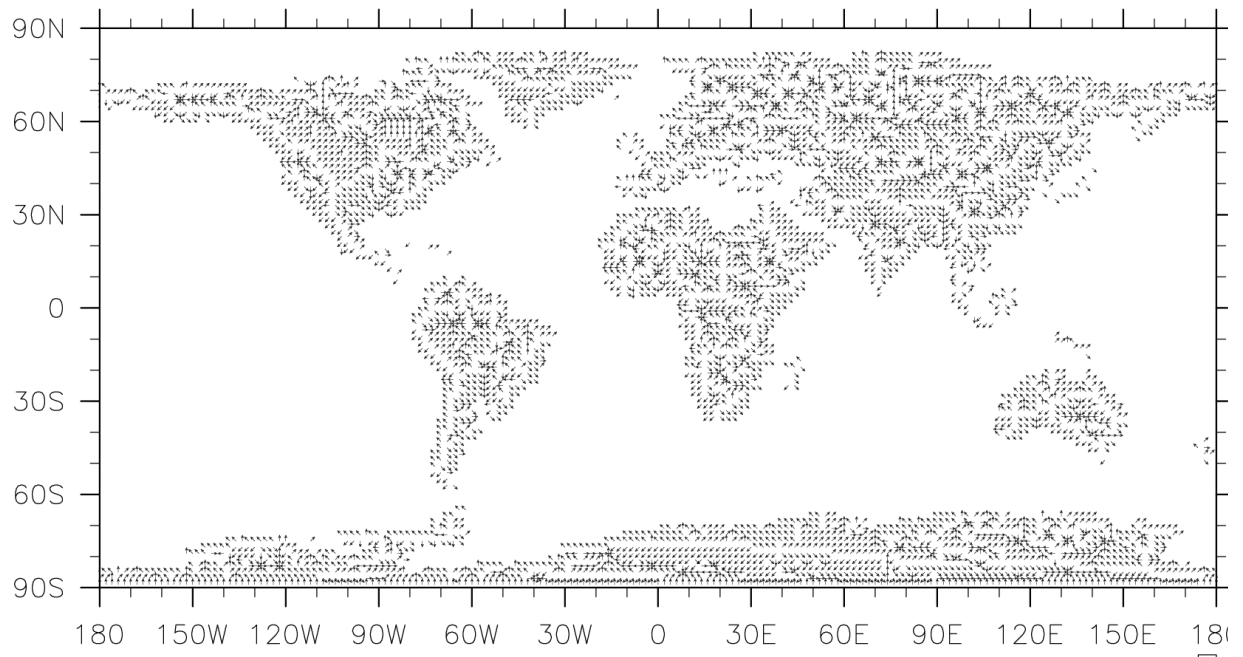
References

Cramer, B. S., K. G. Miller, P. J. Barrett, and J. D. Wright (2011), Late Cretaceous–
Neogene trends in deep ocean temperature and continental ice volume:
Reconciling records of benthic foraminiferal geochemistry (δ18O and Mg/Ca) with
sea level history, *Journal of Geophysical Research: Oceans*, *116*(C12), C12023.

Denk, T., Gri, x, F. msson, Kvac, x30c, and Z. ek (2005), The Miocene floras of Iceland
and their significance for late cainozoic North Atlantic biogeography, *Botanical
Journal of the Linnean Society*, *149*(4), 369-417.

Eldrett, J. S., D. R. Greenwood, I. C. Harding, and M. Huber (2009), Increased
seasonality through the Eocene to Oligocene transition in northern high latitudes,
Nature, *459*(7249), 969-973.

Fretwell, P., et al. (2012), Bedmap2: improved ice bed, surface and thickness datasets
for Antarctica, *The Cryosphere Discuss.*, *6*(5), 4305-4361.

Grímsson, F., T. Denk, and L. A. Símonarson (2007), Middle Miocene floras of Iceland --
the early colonization of an island?, *Review of Palaeobotany and Palynology*,
144(3-4), 181-219.

Hartley, A. (2003), Andean uplift and climate change, *Journal of the Geological Society*,
160(1), 7-10.

Herold, N., M. Huber, and R. D. Müller (2011), Modeling the Miocene Climatic Optimum.
Part I: Land and Atmosphere*, *Journal of Climate*, *24*(24), 6353-6372.

Herold, N., M. Huber, R. D. Müller, and M. Seton (2012), Modeling the Miocene climatic
optimum: Ocean circulation, *Paleoceanography*, *27*(1), PA1209.

Herold, N., M. Seton, R. D. Müller, Y. You, and M. Huber (2008), Middle Miocene tectonic
boundary conditions for use in climate models, *Geochem. Geophys. Geosyst.*,
9(10), Q10009.

Hoorn, C., et al. (2010), Amazonia Through Time: Andean Uplift, Climate Change,
Landscape Evolution, and Biodiversity, *Science*, *330*(6006), 927-931.

Hüsing, S. K., W.-J. Zachariasse, D. J. J. van Hinsbergen, W. Krijgsman, M. Inceöz, M.
Harzhauser, O. Mandic, and A. Kroh (2009), Oligocene–Miocene basin evolution in
SE Anatolia, Turkey: constraints on the closure of the eastern Tethys gateway,
Geological Society, London, Special Publications, *311*(1), 107-132.

Iturralde-Vinent, M. A. (2006), Meso-Cenozoic Caribbean Paleogeography: Implications
for the Historical Biogeography of the Region, *International Geology Review*,
48(9), 791-827.

Karami, M. P. (2011), Paleoceanography of the Miocene Mediterranean Sea and
Paratethys: Regional ocean modelling of the response to closure of the Tethys
Seaway, Utrecht.

Langford, R. P., G. E. Wilford, E. M. Truswell, and A. R. Isern (1995), Palaeogeographic
Atlas of Australia,
http://www.ga.gov.au/resources/multimedia/animation/palaeo/html/palaeo.html,
Australian Geological Survey Organisation, Canberra.

Markwick, P. J. (2007), The palaeogeographic and palaeoclimatic significance of climate
proxies for data-model comparisons, in *Deep-Time Perspectives on Climate
Change: Marrying the Signal from Computer Models and Biological Proxies.*,
edited by M. Williams, Haywood, A.M., Gregory, J. and Schmidt D.N., pp. 251-
312.

Meulenkamp, J. E., and W. Sissingh (2003), Tertiary palaeogeography and
tectonostratigraphic evolution of the Northern and Southern Peri-Tethys platforms
and the intermediate domains of the African–Eurasian convergent plate boundary
zone, *Palaeogeography, Palaeoclimatology, Palaeoecology*, *196*(1–2), 209-228.

Molnar, P. (2008), Closing of the Central American Seaway and the Ice Age: A critical
review, *Paleoceanography*, *23*(2), PA2201.

Montes, C., G. Bayona, A. Cardona, D. M. Buchs, C. A. Silva, S. Morón, N. Hoyos, D. A.
Ramírez, C. A. Jaramillo, and V. Valencia (2012), Arc-continent collision and
orocline formation: Closing of the Central American seaway, *J. Geophys. Res.*,
117(B4), B04105.

Müller, R. D., M. Sdrolias, C. Gaina, and W. R. Roest (2008a), Age, spreading rates, and spreading asymmetry of the world's ocean crust, *Geochem. Geophys. Geosyst.*, *9*(4), Q04006.

Müller, R. D., M. Sdrolias, Gaina C., Steinberger B., and H. C. (2008b), Long-Term Sea-Level Fluctuations Driven by Ocean Basin Dynamics, *Science*, *319*(5868), 1357-1362.

Pekar, S. F., and R. M. DeConto (2006), High-resolution ice-volume estimates for the early Miocene: Evidence for a dynamic ice sheet in Antarctica, *Palaeogeography, Palaeoclimatology, Palaeoecology*, *231*(1-2), 101-109.

Pollard, D., and R. M. DeConto (2009), Modelling West Antarctic ice sheet growth and collapse through the past five million years, *Nature*, *458*(7236), 329-332.

Poore, H. R., R. Samworth, N. J. White, S. M. Jones, and I. N. McCave (2006), Neogene overflow of Northern Component Water at the Greenland-Scotland Ridge, *Geochem. Geophys. Geosyst.*, *7*(6), Q06010.

Robinson, M. M., P. J. Valdes, A. M. Haywood, H. J. Dowsett, D. J. Hill, and S. M. Jones (2011), Bathymetric controls on Pliocene North Atlantic and Arctic sea surface temperature and deepwater production, *Palaeogeography, Palaeoclimatology, Palaeoecology*, *309*(1-2), 92-97.

Shephard, G. E., R. D. Muller, L. Liu, and M. Gurnis (2010), Miocene drainage reversal of the Amazon River driven by plate-mantle interaction, *Nature Geosci*, *3*(12), 870-875.

van Ufford, A. Q., and M. Cloos (2005), Cenozoic tectonics of New Guinea, *AAPG Bulletin*, *89*(1), 119-140.

Weidick, A., R. S. Williams, and J. G. Ferrigno (1995), *Satellite Image Atlas of Glaciers of the World: Greenland*, US Government Printing Office.

Wilson, D. S., and B. P. Luyendyk (2009), West Antarctic paleotopography estimated at the Eocene-Oligocene climate transition, *Geophysical Research Letters*, *36*(16), L16302.

Wilson, D. S., S. S. R. Jamieson, P. J. Barrett, G. Leitchenkov, K. Gohl, and R. D. Larter (2012), Antarctic topography at the Eocene–Oligocene boundary, *Palaeogeography, Palaeoclimatology, Palaeoecology*, *335–336*(0), 24-34.

Wolfe, J. A. (1985), Distribution of major vegetational types during the Tertiary, in *Geophysical Monograph*, edited by E. T. Sundquist and W. S. Broecker, pp. 357-375, American Geophysical Union, Washington, DC.

Zachos, J., M. Pagani, L. Sloan, E. Thomas, and K. Billups (2001), Trends, rhythms, and aberrations in global climate 65 Ma to present, *Science*, *292*(5517), 686-693.